nzsee
NEW ZEALAND SOCIETY FOR EARTHQUAKE ENGINEERING

Influence of failure mode uncertainty on the collapse capacity of RC components

E.A. Opabola & K.J. Elwood
Department of Civil and Environmental Engineering, University of Auckland, Auckland.

ABSTRACT

Acceptance criteria for reinforced concrete components are selected based on the assumption that the failure mode of a component is deterministic. This paper makes a case suggesting that such an assumption may be untrue in certain cases. In this paper, evidences from existing experimental studies supporting the existence of failure mode variability in nominally identical reinforced concrete components are presented. It was observed that failure mode variability in nominally identical components can result in significant variation in collapse capacity. Furthermore, an experimental program on four nominally identical pre-1995 NZ gravity circular columns was presented to further demonstrate the existence of this failure mode variability phenomenon. The failure mode uncertainty phenomenon was linked to the existence of a failure mode transition zone. It is suggested that failure mode uncertainty be adequately treated in the selection of acceptance criteria, development of component fragility functions as well as in probabilistic assessment of global collapse capacity and economic losses.

1 INTRODUCTION

Under seismic demands, RC columns of high-rise structures subjected to significant lateral displacements are expected to dissipate seismic energy without losing their axial load carrying capacity. Post-earthquake reconnaissance reports (e.g. Kam et al. (2011); Sezen et al. (2000)) have attributed the partial or total collapse of RC buildings, subjected to seismic actions, to the failure of gravity columns in these buildings. Under cyclic loading, RC columns exhibit one of three main failure modes namely: flexure-dominated, flexure-shear dominated or brittle shear dominated modes. Brittle shear and flexure-shear dominated modes are characterized by shear distress prior to and after flexural yielding, respectively. For diagonal failure-critical (shear and flexure-shear) components, axial failure may be quite sudden and there is a high likelihood of axial failure occurring immediately after shear failure, especially for components under high axial load (Elwood and Moehle 2005). Flexure-dominated components, however, tend to have a buffer between onset of lateral failure and axial-load failure occurs, especially for low to moderate axial load levels. This can be attributed to the fact that concrete core crushing and significant bar buckling need to occur before the axial load capacity drops below the axial load demand.

During seismic assessment procedures of RC structures, it is typical to assume that the failure mode is deterministic (e.g. ASCE (2018); ATC (2018)). Such a procedure assumes that if nominally identical RC components are tested severally, the same damage mechanism and failure mode is expected and a slight variation in strength and drift capacity due to inherent material uncertainty may be expected.

Recent experimental data have, however, shown that nominally identical components may in fact exhibit different damage mechanisms leading to variability in seismic response. In this paper, a case for the failure mode uncertainty (also referred to as failure mode switch in this paper) in RC components is presented. Results of past experiments are reviewed to show how variation in damage mechanisms between nominally identical reinforced concrete members, leads to variability in drift capacity at axial failure. Furthermore, results from an experimental program conducted to further explore the failure mode switch phenomenon are presented.

2 EXPERIMENTAL EVIDENCE OF FAILURE-MODE SWITCH IN RC COMPONENTS

Results of past experiments were reviewed to show that variation in damage mechanism in nominally identical reinforced concrete members can lead to variability in deformation capacity. Aside from data from laboratory cyclic tests on RC columns, data on monotonic tests on RC beams without web reinforcement were also collated. This is because it is not uncommon finding tests with two or more nominally identical RC beam specimens subjected to the same loading protocol; thus, making these components a good case study. Also, there are similarities in the damage mechanisms of RC beams without web reinforcement and RC columns with widely-spaced transverse reinforcement.

2.1 Causes of failure-mode switch

2.1.1 Strain rate effect

In a series of tests on RC beams, Kulkarni and Shah (1998) have reported a switch from a shear-dominated response at a static strain rate to a flexure-dominated response at a dynamic strain rate. On the other hand, Mutsuyoshi and Machida (1985) have reported a switch from a flexure-dominated response at static strain rate to a shear-dominated response at a dynamic strain rate for nominally identical reinforced concrete columns. Development of an unexpected diagonal failure plane led to reduced deformation capacities (by a magnitude of at least two times) and lower energy dissipation in the column specimens subjected to dynamic strain rates.

Under high strain rates, there is an increase in yield strength of reinforcement and compressive strength of concrete (Seabold 1970). The increase in material strength causes an increase in flexural and shear strength of RC components; however, it can have an adverse effect on the cyclic degradation of strength and stiffness (Wang et al. 2013). The increased rate of cyclic degradation of shear strength generally leads to a higher likelihood of flexure-shear interaction in RC columns under high strain-rate cyclic loading.

2.1.2 Displacement history effect

In their study, Ranf et al. (2004) subjected six nominally identical RC columns to different displacement histories and concluded that while other specimens exhibited a flexure-shear dominated failure mode, one of the specimens exhibited a flexure-dominated response and had a larger drift ratio at axial failure (6%) than the flexure-shear governed specimens(ranging from 3% to 4.75%).

The sensitivity of failure mode to displacement history effect is also likely in RC columns subjected to bidirectional lateral loading. By comparing experimental results of nominally identical circular bridge columns tested using unidirectional lateral loading and bidirectional lateral loading, Wong (1990) deduced that bidirectional loading can cause an unfavourable switch in failure mode from a flexure-dominated failure mode to a flexure-shear dominated failure mode, leading to more severe degradation of stiffness and strength, and subsequently a lower drift capacity. The tests by Wong (1990) were, however, not conducted until axial failure.

2.1.3 Effect of inherent material uncertainty

Xu and Li (2019) subjected nine nominally identical beams without web reinforcement to four-point bending. All nine specimens were tested monotonically under a constant pseudo-static loading rate. The authors observed that four beam specimens exhibited diagonal-tension failure mechanism while the remaining five beams exhibited a flexural mechanism. All the specimens that suffered a diagonal failure had collapse deflection of 10mm while the flexure-dominated beams did not suffer collapse until the end of the test at 50mm deflection. The authors attributed the difference in failure mode to inherent uncertainty in material properties.

Evidence of failure mode switch in RC columns was reported in an experimental study on three non-ductile RC beam-column subassemblies carried out by Motter et al. (2019). The difference between the subassemblies was the spacing in joint reinforcement. The geometric properties, material properties, reinforcement detailing of the columns were nominally identical. The constant axial load on the three specimens was 15% above balanced axial load (P_b). Experimental results showed that failure was localized in the columns only and the load-displacement response was influenced by the variation in failure mode in the columns of the subassemblies. Using experimental data, the authors showed that the joint behaviour did not have any influence on the response of the subassemblies. The failure mechanism of two of the columns was dominated by the formation of a diagonal failure plane and the lateral drifts at axial failure were 2.4% and 3%. The third column experienced a flexure-dominated failure mode and suffered axial failure at 4.85% drift ratio. The authors concluded that the failure mode switch was most likely due to variability in concrete properties within and between columns of test specimens.

3 COMPONENTS SUSCEPTIBLE TO FAILURE-MODE SWITCH

By examining the failure-mode switch cases for columns subjected to cyclic loading, it was noted that the shear capacity ratio (defined as the ratio of flexural shear demand (V_p) to undegraded shear capacity (V_o) computed using the shear strength model proposed by Sezen and Moehle (2004)) of the components were between 0.68 and 0.71. As shown in Figure 1, 0.7 corresponds to the transition point between flexure-shear and flexure failure modes based on the shear strength model proposed by Sezen and Moehle (2004).

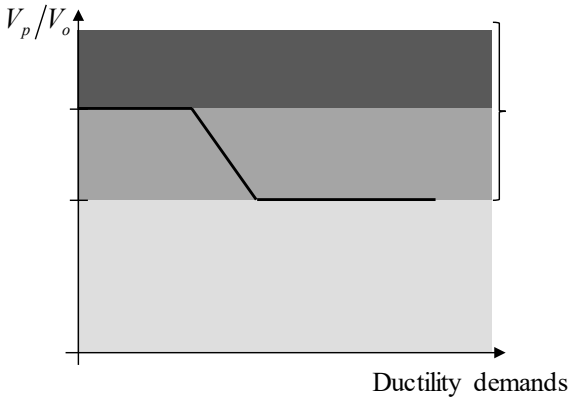

Figure 1: Failure mode classification using shear capacity ratio and transition point between failure modes (NB: The line is defined by k-factor which accounts for degradation of shear capacity with increasing ductility demands)

Using probabilistic tools, Opabola and Elwood (2020) showed that columns with shear capacity ratio other than 0.7, may in fact have a significant likelihood of failure mode switch suggesting that the failure mode transition is not a point but rather a zone. Opabola and Elwood (2020) also showed that the flexure – diagonal failure mode transition zone is bounded by shear capacity ratios of 0.6 and 0.8. The existence of this transition zone is evidenced by the fact that both flexure and flexure-shear failure modes are typically observed in

columns with shear capacity ratio between 0.6 and 0.8 (See Column database by Ghannoum et al. (2015)). Further details are not provided here for the sake of brevity. More information can be sourced from Opabola and Elwood (2020).

4 EXPERIMENTAL PROGRAM

For this experimental program, four full-scale reinforced concrete columns were constructed. The geometric dimensions and reinforcement detailing were selected to be representative of typical detailing of pre-1995 New Zealand reinforced concrete gravity columns without appropriate seismic detailing. From a dataset of 80 reinforced concrete multi-story buildings, built between 1980 and 1995, in Wellington, New Zealand, the geometric dimensions, reinforcement detailing and axial load level on ground floor gravity columns were collated. For designing the columns in this experimental program, the key parameters were column dimension, axial load ratio and transverse reinforcement detailing. Further details on the dataset can be sourced from Puranam et al. (2019).

Following the collation of data from real buildings for the adopted key parameters, a review of past experimental programs was carried out. The ACI 369 column database (Ghannoum et al. 2015), consisting of 319 rectangular columns and 171 circular columns, was reviewed for tests matching the range of parameters identified in the buildings. This review showed the circular columns from the buildings in Wellington were not represented in this dataset. This is due to the fact that past tests on circular columns have typically focused on bridge design configurations. Furthermore, only 11 circular column specimens had a ratio of transverse reinforcement spacing to depth (s/d) larger than 0.5. From this small dataset of lightly reinforced columns, only one column was tested to an axial load level larger than $0.2A_g f'_c$ (where A_g is the gross cross-sectional area of the column and f'_c is the concrete compressive strength). These findings further motivated the need to test circular building columns under high axial loads. To further demonstrate the existence of failure mode switch phenomenon, a decision was made to design the column specimens such that their shear capacity ratio will be equal to 0.7.

4.1 Test specimens

All four RC circular columns specimens were nominally identical with cross-sectional details shown in Figure 2. The columns were tested in double curvature with clear height of 2800mm corresponding to a shear span to depth ratio of 4.1, a longitudinal reinforcement ratio of 1.5% without lap splices, and a wide pitch to the spiral (s/d = 0.7). The decision to test full-scale columns in double curvature was aimed at eliminating uncertainties due to simplifications of in-situ conditions (e.g. boundary conditions, scale effect, location of point of contra flexure). Each specimen was cast with top and bottom rigid blocks to simulate rigid beam-column joints or foundation. The rigid blocks were designed to remain elastic during the tests.

The mean measured compressive strength for column concrete was 31MPa from standard compression tests on 100 x 200 mm cylinders. The longitudinal reinforcement bars were Grade 300 deformed bars, representative of older-type structures, with a measured mean yield strength (f_y) of 320 MPa and ultimate strength of 451MPa. The plain round spirals, used as transverse reinforcement, did not have a definite yield point because bars of smaller diameters are typically stored in coil form; thus, the yield point and yield plateau are lost when the bars were straightened. The column spirals had measured mean yield (0.2% proof stress) and ultimate strengths of 359MPa and 485.5MPa, respectively.

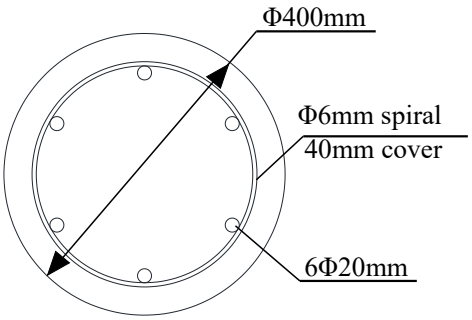

Figure 2: Cross-sectional details of column specimens

4.2 Test set-up

The tests were conducted at the Structures Test Hall of the University of Auckland using a test system designed for double curvature column testing (Figure 3). An out-of-plane pantograph system was designed to restrict out-of-plane deformations of the column specimens. Global deformations in the specimen and loading frame were measured and monitored throughout the test. A total of 40 instrumentations were used. 15 string potentiometers were used in measuring lateral (in-plane and out-of-plane) and axial deformations of the columns. On one face of the column, deformation on both top and bottom portions of the column were measured using an array of displacement gauges and linear potentiometers.

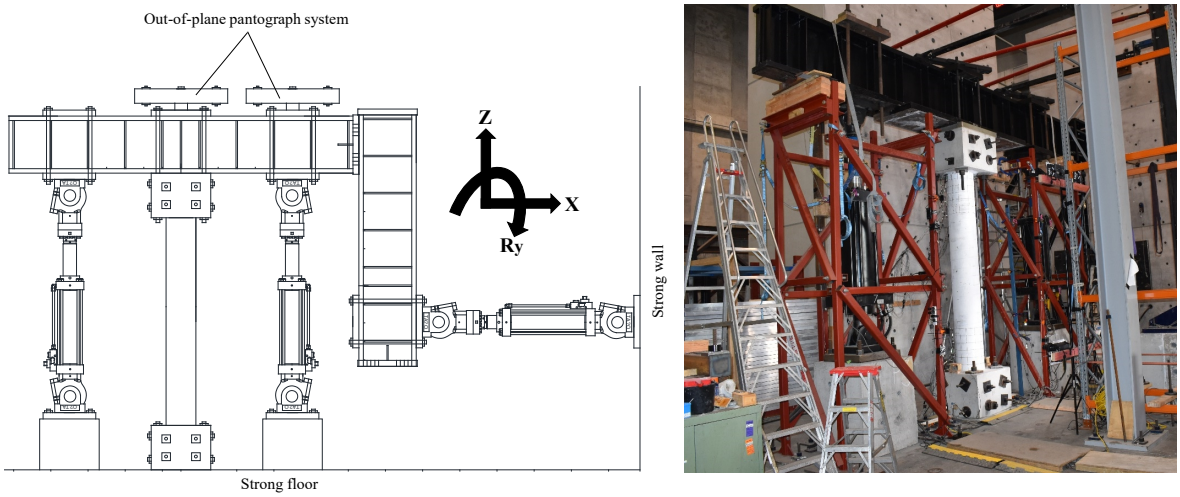

(a) (b)

Figure 3: Test set-up

4.3 Loading protocol

A representative axial load (N) of 1650kN ($0.42A_g f'_c$) was applied to all specimens. The applied axial load is equivalent to $1.1P_b$, making the column specimens compression-controlled. The plastic shear demand and un-degraded shear capacity (based on Sezen and Moehle (2004) shear model) for the columns are 138kN and 196kN, respectively; giving a shear capacity ratio of 0.7.

Following the aim of the study, two specimens (Specimen 2 and 3) were subjected to the same loading protocol to investigate replicability of test results. The adopted loading protocol is similar to the standard type loading protocol (Figure 4a). The loading protocol of Specimen 1 was initially intended to be similar to Specimens 2 and 3; however, once the upper portion of the column experienced plastic hinging during unloading at +1.5% drift, the vertical actuators could not satisfy constraints of the mixed-mode control (applying constant axial load and ensuring zero rotation of the loading frame), thus triggering vibrations in the vertical actuators. Rather than continue with the standard loading protocol, it was decided to unload Specimen 1 to zero lateral force and

then subject it to a monotonic push until failure. To avoid this instability in subsequent tests, the loading rate of the horizontal actuator was reduced to 0.05mm/sec from the initial 0.2mm/sec; giving the actuators sufficient buffer time to respond to the mixed-mode control strategy.

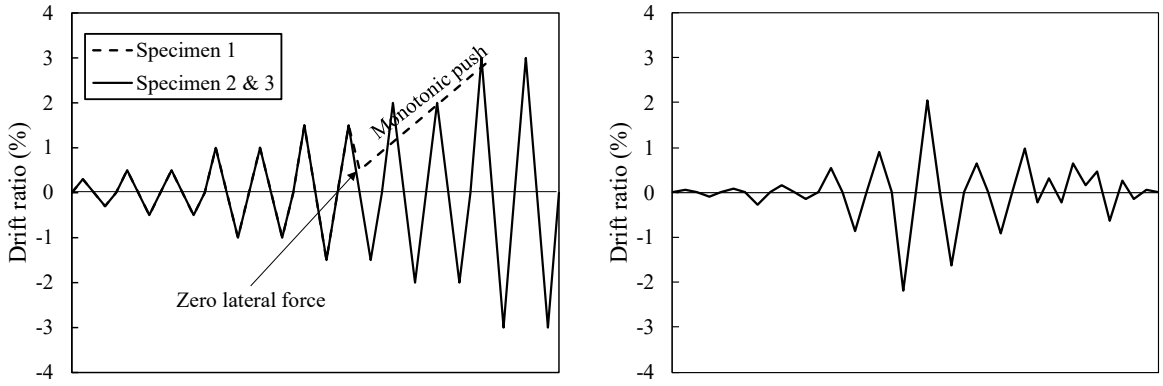

(a) (b)

Figure 4: (a) Displacement protocol for Specimens 1, 2 and 3. (b) Displacement protocol for Specimen 4

The displacement protocol for Specimen 4 matched that used by Motter et al. (2019). This displacement history was adopted in the current study as it was deemed to be a sufficient representation of displacement history on a typical ground floor column of a RC building subjected to a near-fault type seismic event and allowed comparison of results between the current study and Motter et al. (2019).

For all specimens, following initial axial failure (defined as the point when the column could no longer carry the initial axial load demand), the column was held in this position under a displacement control constraint. Axial load was then re-applied using the vertical actuators in displacement control (a displacement-control regime was favored a load-control regime for safety precautions). The residual axial capacity was defined as the point when the load cell readings of the vertical actuators stopped increase under axial compression.

4.4 Observed damage and hysteretic response

The damage states of all specimens at the end of the tests are presented in Figures 5, 6, 7 and 8. As shown in the Figures, there is significant variability in the damage mechanism of the specimens. Specimens 1 and 3 exhibited a flexure-dominated mechanism characterised by concrete spalling and bar buckling. The responses of Specimens 2 and 4 were dominated by the development of a critical diagonal plane and axial failure in these specimens was very brittle and sudden. For the sake of brevity, no information is provided on damage progression in all specimens.

(a) Top section (b) Bottom section

Figure 5: Photo of Specimen 1 after axial failure and removal of loose concrete

Axial failure in Specimens 2 and 4 was due to a lack of shear transfer along the critical diagonal failure plane. The buckled bars in Specimen 2 (See Figure 6) also suggest that the dowel resistance of these bars had degraded significantly and was not sufficient to carry the applied axial load. Following axial failure, the measured residual axial capacity (defined previously) of the specimens were 201kN and 348kN respectively (Table 1). In Specimens 1 and 3, axial failure was as a result of continuous cover spalling, concrete core disintegration as well as longitudinal reinforcement buckling which reduced the axial capacity till it was lesser than the axial load demand. The two specimens, however, had larger levels of residual axial capacity (defined previously) of 647kN and 529kN respectively. The force-displacement responses of all four specimens are presented in Figure 9. Table 1 provides a summary of key force-displacement parameters. The peak strength in all specimens are similar. This is expected as the specimens are nominally-identical.

(a) Diagonal cracking (b) Top section (c) Bottom section

Figure 6: Damage mechanism of Specimen 2

Although all specimens had similar drift capacities at onset of loss of lateral resistance, defined as 20% loss in maximum lateral resistance, there was more noticeable difference in drifts at loss of initial axial load capacity. As shown in Table 1, in comparison to drift capacity at lateral failure, there is a significant variation in the measured drift capacity at axial failure. This is attributed to a larger influence of displacement history and damage mechanism on the drift capacity at axial failure.

(a) Top section (b) Bottom section

Figure 7: Photo of Specimen 3 after axial failure and removal of loose concrete

Similar to conclusions from tests on columns with moderate level of axial load (Melek and Wallace 2004; Sezen and Moehle 2006), the collapse capacity of the compression-controlled columns is displacement-history dependent. In order to account for correlation in damage mechanism, Specimen 2 is compared with Specimen 4 (both specimens developed a diagonal failure plane) while Specimen 3 is compared with Specimen 1 (both specimens were flexure-governed). As shown in Table 1, specimens subjected to a near-fault type displacement protocol have a drift capacity at axial failure about 50% larger than specimens subjected to standard cyclic protocol. According to experimental data, the influence of displacement history on drift capacity at axial failure is not negligible.

(a) Critical failure plane (b) Top section (c) Bottom section

Figure 8: Damage mechanism of Specimen 4

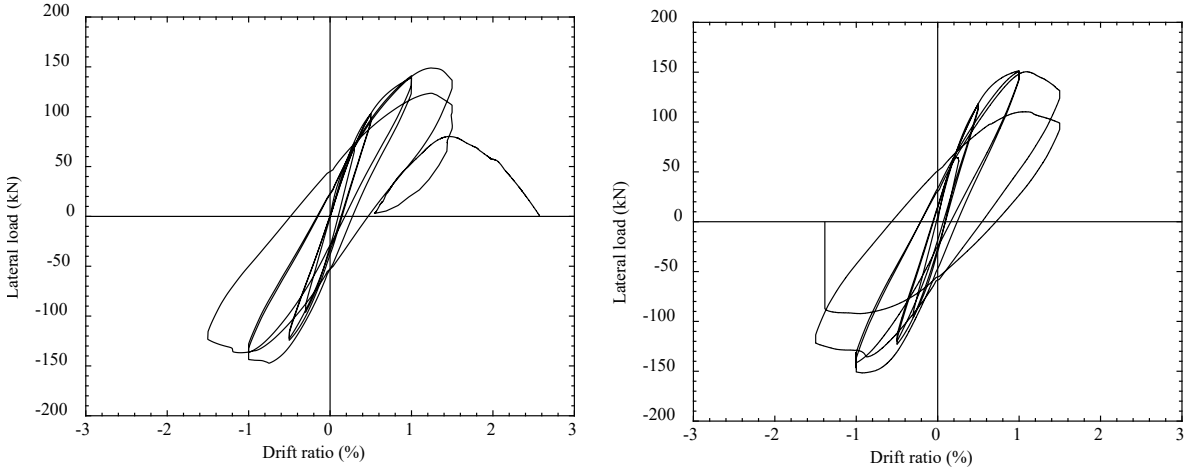

(a) Specimen 1 (b) Specimen 2

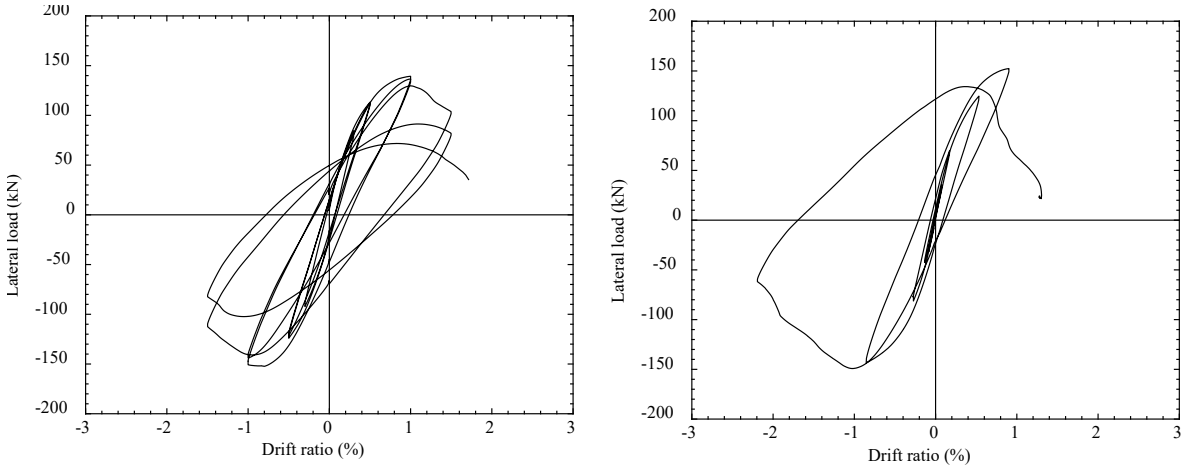

(c) Specimen 3 (d) Specimen 4

Figure 9: Hysteretic response of column specimens

Table 1: Summary of measured key displacement parameters (NB: NF: Near-fault; SP: Standard loading protocol)

s/no	Specimen	Loading protocol	Failure mode	$\theta_{0.8Vmax}$ (%)	NF/SP	θ_a (%)	NF/SP	Residual axial capacity (kN)
1	Specimen 1	Near-fault	Flexure	1.5	1.05	2.56	1.49	647
	Specimen 3	Standard		1.42		1.72		529
2	Specimen 4	Near-fault	Flexure-shear	1.49	0.99	2.19	1.46	348
	Specimen 2	Standard		1.5		1.5		201

5 EFFECT OF FAILURE MODE SWITCH ON COLLAPSE CAPACITY OF RC COLUMNS

Experimental results from all studies represented in Section 2 show the buffer between drifts at axial failure and lateral failure is larger in flexure-dominated columns when compared with nominally identical flexure-shear critical columns. This buffer, however, is sensitive to axial load. Figure 10 shows this buffer for three experimental programs – current study with axial load ratio ($N/A_g f'_c$) of 0.42, Ranf et al. (2004) with axial load ratio of 0.1 and (Motter et al. 2019) with axial load ratio of 0.37. As axial load increased, irrespective of failure mode, the buffer reduced (Figure 10). Likewise, the potential influence of variability in failure on drift at axial failure is reduced with increase in axial load.

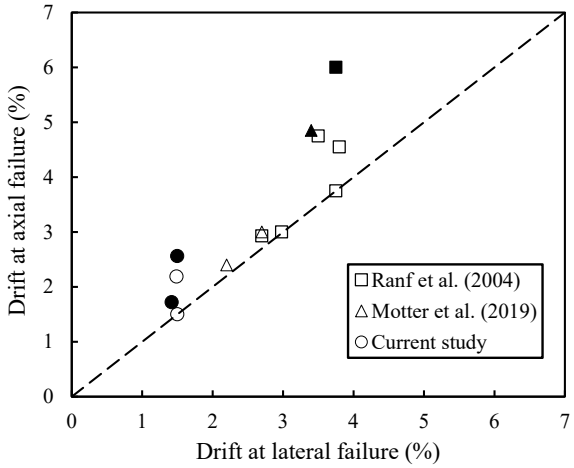

Figure 10: Influence of failure mode on buffer between lateral and axial failure (symbols for flexure-critical columns are filled, shear-critical columns are open)

For components in the transition zone, as defined by Opabola and Elwood (2020), the tendency of exhibiting two different failure modes and its effect on global collapse capacity warrants the need to account for this uncertainty in the development of acceptance criteria. Typically, acceptance criteria are selected either by using a unified target failure probability, for each performance objective, without consideration of failure mode (as adopted in ASCE/SEI 41-17) or different target failure probabilities for different failure modes by recognising the step change in component response. This procedure attaches lower target probabilities to brittle failure modes where a higher level of safety margin is necessary. For components in the transition zone, the influence of failure mode variability can be incorporated in the evaluation of refined target probabilities, accounting for the likelihood of failure mode variability, which is then used in selecting appropriate multipliers to drift capacity median estimates. Further information on this can be sourced from Opabola and Elwood (2020).

6 SUMMARY AND CONCLUSIONS

Experimental studies have shown that nominally identical test specimens may exhibit different failure modes due to inherent material uncertainty, loading rate or displacement history. Aside from the larger drift at axial failure, a flexure-dominated component may have a larger residual axial capacity than a nominally identical diagonal-failure critical component. The effect of failure mode on collapse capacity variability is, however, sensitive to axial load. At high axial load, the effect may be minimal.

Experimental results also show that columns subjected to near-fault type loading protocol tend to have drift at axial failure larger than columns subjected to standard type protocol. The difference between displacement demand when loss of lateral capacity and axial failure occurs is also sensitive to loading protocol. Further studies, aimed at understanding the buffer till axial failure following loss of lateral strength need to be carried out.

It is suggested the failure-mode switch phenomenon be accounted for in the selection of acceptance criteria and development of future fragility functions for components susceptible to failure mode variability. Likewise, future research studies should consider the influence of failure mode uncertainty at the subassembly level (e.g. beam-column connections) and system level (e.g. frames) when assessing seismic collapse probability.

REFERENCES

ASCE. (2017). *Seismic Evaluation and Retrofit of Existing Buildings*. American Society of Civil Engineers, Reston, VA.

ATC. (2018). *Seismic Evaluation of Older Concrete Frame Buildings for Collapse Potential*. Applied Technology Council for the Federal Emergency Management Agency, Washington, D.C.

Elwood, K. J., and Moehle, J. P. (2005). "Axial capacity model for shear-damaged columns." *ACI Structural Journal*, 102(4), 578–587.

Ghannoum, W., Sivaramakrishnan, B., Pujol, S., Catlin, A. C., Fernando, S., Yoosuf, N., and Wang, Y. (2015). "NEES: ACI 369 Rectangular Column Database." <https://datacenterhub.org/resources/255>.

Kam, W. Y., Pampanin, S., and Elwood, K. (2011). "Seismic performance of reinforced concrete buildings in the 22 February Christchurch (Lyttelton) earthquake." *Bulletin of the New Zealand Society for Earthquake Engineering*, 44(4), 239–278.

Kulkarni, S. M., and Shah, S. P. (1998). "Response of reinforced concrete beams at high strain rates." *ACI Structural Journal*, 95(6), 705–715.

Melek, M., and Wallace, J. W. (2004). "Cyclic behavior of columns with short lap splices." *ACI Structural Journal*, 101(6).

Motter, C. J., Opabola, E., Elwood, K. J., and Henry, R. S. (2019). "Seismic Behavior of Nonductile Reinforced Concrete Beam-Column Frame Subassemblies." *Journal of Structural Engineering*, 145(12), 04019157.

Mutsuyoshi, H., and Machida, A. (1985). "Behavior of Reinforced Concrete Members Subjected to Dynamic Loading (Reprint from Transactions of JSCE, Vol. V-2, No.354, 1985)." V(6), 51–68.

Opabola, E. A., and Elwood, K. J. (2020). "Incorporating Failure Mode Uncertainty into Probabilistic Assessment of RC Components." *Structural Safety*, (Accepted).

Puranam, A., Filippova, O., Pastor-paz, J., Stephens, M., Elwood, K. J., Ismail, N., Noy, I., and Opabola, E. (2019). "A Detailed Inventory Of Medium - to High-Rise Buildings in Wellington's Central Business District." 52(4), 172–192.

Ranf, R. T., Eberhard, M. O., and Stanton, J. F. (2004). "Effects of Displacement History on Failure of Lightly Confined Bridge Columns." *ACI Special Pubblication*, SP-236-2, 23–42.

Seabold, R. H. (1970). *Dynamic shear strength of reinforced concrete beams. Part 3*. Naval Civil Engineering Lab Port Hueneme CA.

Sezen, H., Elwood, K. J., Whittaker, A. S., Mosalam, K. M., Wallace, J. W., and Stanton, J. F. (2000). "Structural Engineering Reconnaissance of the August 17, 1999, Kocaeli (Izmit), Turkey, Earthquake." *Technical Rep. No., PEER 2000, 9*.

Sezen, H., and Moehle, J. P. (2004). "Shear Strength Model for Lightly Reinforced Concrete Columns." *Journal of Structural Engineering*, 130(11), 1692–1703.

Sezen, H., and Moehle, J. P. (2006). "Seismic tests of concrete columns with light transverse reinforcement." *ACI Structural Journal*, 103(6), 842–849.

Wang, D., Li, H. N., and Li, G. (2013). "Experimental tests on reinforced concrete columns under multi-dimensional dynamic loadings." *Construction and Building Materials*, Elsevier Ltd, 47, 1167–1181.

Wong, Y. L. (1990). "Squat Circular Bridge Piers Under Multi-directional Seismic Attack." PhD thesis, University of Canterbury.

Xu, T., and Li, J. (2019). "Experimental investigations of failure modes of reinforced concrete beams without web reinforcement." *Engineering Structures*, Elsevier, 185(September 2018), 47–57.